IEICE TRANS. FUNDAMENTALS, VOL.E98–A, NO.1 JANUARY 2015

PAPER

Application of the recursive transfer method to flexural waves II: Reflection enhancement caused by resonant scattering in acoustic waveguide

Hatsuhiro KATO[†a)], *Member*, **Hatsuyoshi KATO**[††], *Nonmember*, *and* **Takaaki ISHII**[†], *Member*

SUMMARY Resonant scattering of flexural waves in acoustic waveguide is analysed by using the recursive transfer method (RTM). Because flexural waves are governed by a fourth-order differential equation, a localized wave tends to be induced around the scattering region and dampening wave tails from the localized wave may reach the ends of a simulation domain. A notable feature of RTM is its ability to extract the localized wave even if the dampening tail reaches the end of the simulation domain. Using RTM, the enhanced reflection caused by a localized wave is predicted and the shape of the localized wave is explored at its resonance with the incident wave.

key words: *Recursive transfer method, Flexural wave, Elastic plate, Fano resonance, Weak-form discretization*

1. Introduction

Recursive transfer method (RTM) is a numerical method for analysing electron waves [1], [2] and has been extended to the microwave scattering [3]–[6]. However, the phenomena to which RTM is applicable has been limited to systems that are governed by a second-order differential equation [7]; flexural waves on elastic plates have not previously been considered because those are governed by a fourth-order differential equation. In a previous paper (hereafter paper I), we developed a new discretization scheme, *i.e.* the *weak-form discretization scheme*, that is applicable even to flexural waves to derive a second-order difference equation [8]. The accuracy of the derived equation was also confirmed by comparing with mode shapes obtained by an analytical expression. However, the validity of RTM for analysing a scattering problem of flexural waves still remains to be demonstrated. In this study, we apply RTM to the derived second-order difference equation to solve a scattering problem.

Various surface waves on solids are used to realize elastic wave devices [9], [10]. Acoustic waveguides made of a thin elastic plate provide a favourable research target because the flexural waves can be controlled by adjusting geometrical parameters [11]. Moreover, various waveguide shapes can be formed with lithographic technology and material constants such as Young's modulus can be modulated by implanting impurities [12].

The motion of flexural waves on a homogenous plate is governed by a fourth-order differential equation that has a biharmonic term expressed with double Laplacians [13], [14]. For inhomogeneous plates, two additional operators are necessary as pointed out in paper I. Therefore, the theoretical framework of RTM has to be extended for adapting to the modulated governing equation.

Here we propose a new procedure for formulating absorbing boundary condition (ABC) using the stepping matrix that is defined in the RTM procedure. The proposed ABC numerically realizes matching between waves in scattering and input/output regions. Unlike perfectly matched layers (PML) [15], [16] no extra layer is needed. The origin of the numerically matching concept can be traced back to Ref. [17]. Although the analytic formulation of PML has also been extended to elastic systems [18], [19] and to systems with near fields [20], our ABC provides another utility tool that can be applied systems possessing localized waves with dampening tails.

A waveguide system governed by a second-order differential equation does have the travelling mode, but it does not always have the dampening/growing waveguide mode. In contrast, a flexural wave system in acoustic waveguides always has the additional dampening/growing mode as discussed in Kirchhoff plate theory [21], because the governing differential equation is fourth-order. Using the freedom of the dampening/growing modes, the scattering wave can induce a localized wave with dampening tails. Moreover, resonance between the localized wave and the incident wave can occur.

In a system composed of quantum dots with lead lines [22], the localized wave or quasi-localized wave causes Fano resonance [23] in which the resonance curve is asymmetric and the transmission rate may vanish. In this study, the similar resonance appears in acoustic waveguides with a step-like region to serve as the scattering region. A notable feature of the resonance is full reflection that is assisted by the localized wave.

The organization of the present paper is as follows. In Sec. 2, the second-order difference equation governing flexural waves is introduced, and the RTM procedure is adapted for solving the problem of flexural waves. In Sec. 3, resonant scattering in an acoustic waveguide with a partially

Manuscript received April **, 2012.

[†]The author is with the Interdisciplinary Graduate School of Medicine and Engineering, University of Yamanashi, Takeda, 4-3-11, Kofu, Yamanashi, 400-8511 Japan.

[††]The author is with the Tomakomai National College of Technology, 433, Nishikioka, Tomakomai, Hokkaido, 059-1275, Japan.

a) E-mail: katoh@yamanashi.ac.jp

DOI: 10.1587/transfun.E98.A.354

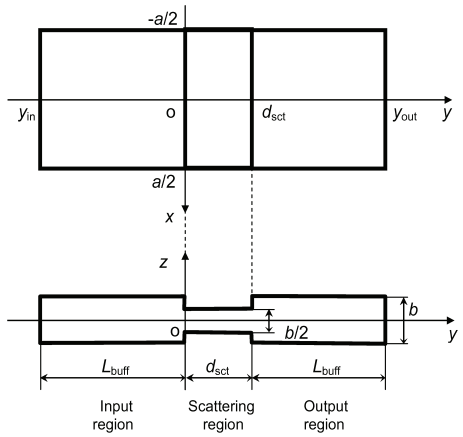

Fig. 1 Schematics of an acoustic waveguide composed of three regions: Scattering region $0 < y < d_{sct}$, input region $y_{in} < y < 0$ and output region $d_{sct} < y < y_{out}$.

thinned part is analysed with RTM. The reflection can possibly enhance the resonance in which a localized wave induced in the scattering region plays an important role. Section 4 is devoted to conclusions. The accuracy of RTM and the relation to the finite element method (FEM) are discussed in Appendixes A and B, respectively.

2. RTM for flexural waves

2.1 Difference equation governing flexural waves

Figure 1 shows a schematic of an acoustic waveguide made of a thin elastic plate with the uniform width a; the vertical scale is exaggerated for clarity. The central thin part is the scattering region where the plate thickness is uniform, but the present formulation is valid even if the thickness depends on the coordinates provided that inversion symmetry is maintained along the z-axis. The x- and y-coordinates are set along the width and direction of propagation, respectively. The origin of the z-axis is assumed to be at the centre of the plate thickness, then the plate surfaces are located at $z = \pm b(x,y)/2$. The input and output ends or the lower and upper limits of the simulation domain are placed at $y = y_{in}$ and $y = y_{out}$, respectively. The plate is assumed to be so thin that displacements perpendicular to the plate are determined by flexural motions. The incident wave is supplied from the end at $y = y_{in}$ and is scattered in the region $0 < y < d_{sct}$ where the plate thickness is thinner than in other regions. Ultimately, the incident wave induces a reflected wave and a transmitted wave, which pass through the ends of the simulation domain at $y = y_{in}$ and $y = y_{out}$, respectively.

In paper I, it was shown that the flexural waves on a thin elastic plate are governed by the following differential equation,

$$\Delta_0(D_0\Delta_0 u) + \Delta_1(D_1\Delta_1 u) + \Delta_2(D_2\Delta_2 u) - \rho I\omega^2\Delta_0 u - \rho b\omega^2 u = 0, \quad (1)$$

if the waves are in a steady state with an angular frequency ω. Here $u(x,y)$ is the vertical displacement of plate, ρ is a mass density, $I(x,y) = b(x,y)^3/12$ is a moment of inertia, $D_0(x,y) = (1+\nu)Eb(x,y)^3/24$ and $D_1(x,y) = D_2(x,y) = (1-\nu)Eb(x,y)^3/24$ with Young's modulus E and Poisson's ratio ν. The operators Δ_0, Δ_1 and Δ_2 are defined as follows: $\Delta_0 = \frac{\partial^2}{\partial x^2} + \frac{\partial^2}{\partial y^2}$, $\Delta_1 = \frac{\partial^2}{\partial x^2} - \frac{\partial^2}{\partial y^2}$ and $\Delta_2 = 2\frac{\partial^2}{\partial x \partial y}$. Futhermore, the differential equation was transformed into a second-order difference equation by applying the weak-form discretization scheme as follows:

$$\bar{c}_n\mathbf{\Phi}(y_{n-1}) + \bar{b}_n\mathbf{\Phi}(y_n) + \bar{a}_n\mathbf{\Phi}(y_{n+1}) = 0. \quad (2)$$

Here, the interval $y_{in} \le y \le y_{out}$ is divided into N_y parts with the step size $h_y = (y_{out} - y_{in})/N_y$ and the interval $-a/2 \le x \le a/2$ is divided into N_x parts with the step size $h_x = a/N_x$. Then, the spatial coordinates are discretized as follows:

$$y_n = y_0 + nh_y, \quad (3)$$

$$x_\ell = x_0 + \ell h_x, \quad (4)$$

where the initial values are defined by $y_0 = y_{in}$ and $x_0 = -a/2$. The indices n and ℓ vary as $n = 0, 1, 2, ..., N_y$ and $\ell = 0, 1, 2, ..., N_x$, respectively. Using the plate displacement $u(x.y)$ and its derivatives at $(x,y) = (x_\ell, y_n)$, the four-dimensional vector $\mathbf{U}_{n\ell}$ is defined by

$$\mathbf{U}_{n\ell} = [u(x_\ell, y_n)\ u_y(x_\ell, y_n)\ u_x(x_\ell, y_n)\ u_{xy}(x_\ell, y_n)]^T, \quad (5)$$

where the subscripts x and y on the variable $u(x,y)$ denote the derivatives with respect to x and y, respectively. The field variable $\mathbf{\Phi}(y_n)$ in the difference equation (2) is a $4(N_x+1)$-dimensional column vector that is composed of four-dimensional vectors as follows:

$$\mathbf{\Phi}(y_n) = \{\mathbf{U}_{n\ell}\}. \quad (6)$$

Here, the brackets, { }, indicate a shortened expression in which the index ℓ varies over its whole range $\ell = 0, 1, ..., N_x$. The coefficients $\bar{c}_n$, $\bar{b}_n$ and $\bar{a}_n$ are $4(N_x+1) \times 4(N_x+1)$ matrices whose definitions were given in paper I. All properties of plates are reflected in these coefficients.

2.2 Stepping matrices and waveguide modes

The stepping matrix $\bar{S}_n$ is a type of transfer matrix that propagates the field vector $\mathbf{\Phi}(y_n)$ by one step as follows [1]:

$$\mathbf{\Phi}(y_{n+1}) = \bar{S}_n\mathbf{\Phi}(y_n). \quad (7)$$

Shifting the index n to $n-1$ in this relation and letting $\mathbf{\Phi}(y_{n-1}) = \bar{S}_{n-1}^{-1}\mathbf{\Phi}(y_n)$, it is easily to derive the recursive relation for $\bar{S}_n$ from the difference equation (2) ,

$$\bar{S}_{n-1} = -(\bar{a}_n\bar{S}_n + \bar{b}_n)^{-1}\bar{c}_n. \quad (8)$$

If the boundary value $\bar{S}_{N_y}$ at the end $n = N_y$ is known, then all values $\bar{S}_n$ ($n = N_y-1, N_y-2, , ..., 2, 1, 0$) can be successively determined by using the recursive relation.

When a flexural wave takes a waveguide mode at the input/output region adjacent to the scattering region, the wave is expressed as $u(x,y) = X(x)e^{\gamma y}$ with mode function

$X(x)$. Here, η is a propagation constant whose real and imaginary parts are the dampening/growing factor and the wave number, respectively. The waveguide mode can also be expressed in discrete fashion using the column vector $\mathbf{\Phi}(y_n)$ with a constant λ and a vector $\mathbf{\Phi}_X$ as follows:

$$\mathbf{\Phi}(y_n) = \lambda^n \mathbf{\Phi}_X. \tag{9}$$

Since the continuous and discrete expressions are for the same wave guide mode, we can regard as $\lambda \approx e^{\eta h_y}$. For a plane wave on an infinitely broad homogenous plate, we estimated in Appendix A that the error of this approximation is of order h_y^4 in magnitude.

Substituting (9) for $\mathbf{\Phi}(y_n)$ in the governing equation (2) yields

$$(\lambda^{-1}\bar{c}_{\rm wg} + \bar{b}_{\rm wg} + \lambda\bar{a}_{\rm wg})\mathbf{\Phi}_X = 0, \tag{10}$$

which defines a type of the eigenvalue problem with an eigenvalue λ and eigenvector $\mathbf{\Phi}_X$. Here, the coefficients $\bar{c}_{\rm wg}$, $\bar{b}_{\rm wg}$ and $\bar{a}_{\rm wg}$ are values of $\bar{c}_n, \bar{b}_n$ and $\bar{a}_n$ for the translationally invariant input/output region in a uniform waveguide, and are independent of the discrete site index n. The condition (10) can be transformed into an eigenvalue problem defined by the following equation

$$\begin{bmatrix} \bar{c}_{\rm wg} & \frac{1}{2}\bar{b}_{\rm wg} \\ \bar{O} & \bar{I} \end{bmatrix} \begin{bmatrix} \mathbf{\Phi}_X \\ \mathbf{\Psi}_X \end{bmatrix} = -\lambda \begin{bmatrix} \frac{1}{2}\bar{b}_{\rm wg} & \bar{a}_{\rm wg} \\ -\bar{I} & \bar{O} \end{bmatrix} \begin{bmatrix} \mathbf{\Phi}_X \\ \mathbf{\Psi}_X \end{bmatrix}. \tag{11}$$

Here, the column vector $\mathbf{\Psi}_X$ is defined by $\mathbf{\Psi}_X = \lambda\mathbf{\Phi}_X$, the matrices $\bar{O}$ and $\bar{I}$ are the zero matrix and identity matrix of $4(N_x+1)\times 4(N_x+1)$, respectively.

For an electron wave that is described by a second-order differential equation, the coefficients satisfy the symmetric relation $\bar{a}_{\rm wg} = \bar{c}_{\rm wg}$ and the dimension of the eigenvector is N_x [3]. In the present case of flexural waves, the symmetric relation for the coefficients becomes to $\bar{c}_{\rm wg}\Upsilon = \Upsilon\bar{a}_{\rm wg}$, where the matrix Υ is defined as $\Upsilon = [-(-1)^j\delta_{ji}]$ with the Kronecker delta δ_{ij}. This relation is derived by the y-axis inversion where the field vector is transformed by $\mathbf{\Phi} \to \Upsilon\mathbf{\Phi}$. The dimension of the eigenvector is eight times larger than that for electron waves. This extension of the vector dimension is ultimately caused by the fact that flexural waves are described by a fourth-order differential equation.

Since the eigenvalues are obtained from the eigenvalue problem (11), the number of those is $8(N_x+1)$; the eigenvalues can be numbered with the index q (= 1, 2, ..., $8(N_x+1)$) as $\lambda_q = e^{\eta_q h_y}$, and the eigenvectors are also given by $[\mathbf{\Phi}_q\ \mathbf{\Psi}_q]^T$. Here, $\mathbf{\Psi}_q = \lambda_q\mathbf{\Phi}_q$ and the parameter $\eta_q(=\gamma_q+ik_q)$ is a propagation constant. When $\mathrm{Re}[\eta_q](=\gamma_q) = 0$, the waveguide mode defined by the eigenvector is a travelling wave and the sign of $\mathrm{Im}[\eta_q](=k_q)$ indicates the travelling direction. For a travelling wave with positive k_q, the wave advances in the positive direction of the y-axis and vice versa for negative k_q. Reflected and transmitted waves can be expanded as travelling waves. Furthermore, when $\gamma_q \neq 0$, the sign of γ_q indicates the dampening/growing rate of the wave amplitude along the y-axis. The dampening/growing waveguide eigenmodes can be used to express the wave tail which penetrates into the input/output region from the scattering region.

If the quantity η_q is a propagation constant, the inverted quantity $-\eta_q$ and the complex conjugate η_q^* are also propagation constants because of y-axis inversion and time-reversal symmetry, respectively. Therefore, if a propagation constant is expressed as $\eta_q = \gamma_q + ik_q$, corresponding four values given by $\pm\gamma_q \pm ik_q$ with all combinations of the two double signs are also propagation constants.

Using the freedom to choose the double signs in $\pm\gamma_q \pm ik_q$, we can choose a set of $4(N_x+1)$ propagation constants so as to satisfy $\mathrm{Im}[\eta_{a_j}] > 0$ for travelling wave modes ($\mathrm{Re}[\eta_{a_j}] = 0$) and $\mathrm{Re}[\eta_{q_j}] < 0$ for non-travelling wave modes ($\mathrm{Re}[\eta_{a_j}] \neq 0$). We label these with the index j (= 1, 2, 3, ..., $4(N_x+1)$): the corresponding eigenvectors $\mathbf{\Phi}_{q_j}$ are also labelled with the same index j. Now, the matrix $\bar{K}_+^{(\rm dmp)}$ is introduced such that

$$\bar{K}_+^{(\rm dmp)} = \bar{T}[e^{\eta_{q_j}h_y}\delta_{ji}]\bar{T}^{-1}, \tag{12}$$

using the modal matrix $\bar{T}$ defined by

$$\bar{T} = [\mathbf{\Phi}_{\lambda_{q_1}}\ \mathbf{\Phi}_{\lambda_{q_2}}\ \mathbf{\Phi}_{\lambda_{q_3}}\ \ldots\ \mathbf{\Phi}_{\lambda_{q_{4(N_x+1)}}}], \tag{13}$$

then the matrix $\bar{K}_+^{(\rm dmp)}$ serves as the stepping matrix that satisfies the recursive relation (8). If the stepping matrix $\bar{K}_+^{(\rm dmp)}$ operates on the field vector $\mathbf{\Phi}(y_n)$, the modal matrix $\bar{T}^{-1}$ decomposes $\mathbf{\Phi}(y_n)$ into wave components of travelling and non-travelling waves. Furthermore, it propagates those wave components by one step as a travelling wave towards the positive direction or as a dampening wave according to whether the components are travelling or non-travelling.

In a similar manner, three other variants such as $\bar{K}_-^{(\rm dmp)}$, $\bar{K}_+^{(\rm grw)}$ and $\bar{K}_-^{(\rm grw)}$ can be defined. Here, the subscript, $\pm$, indicates the direction to which the travelling wave components proceed. The superscript, dmp/grw, indicates whether the tail of the localized wave component is dampening or growing along the positive direction of the y-axis.

2.3 ABC and the scattering problem

2.3.1 Waves in input/output regions

Assuming that the waveguide continues in the regions $y < y_1(= y_{\rm in} + h_y)$ and $y > y_{N_y}(= y_{\rm out})$, the range of the discrete index n is allowed to take negative values and the integer values over N_y. Then, the field variable $\mathbf{\Phi}(y_n)$ can be expressed in terms of the stepping matrices as

$$\mathbf{\Phi}(y_n) = \begin{cases} \left(\bar{K}_+^{(\rm dmp)}\right)^n \mathbf{\Phi}_{\rm in} + \left(\bar{K}_-^{(\rm grw)}\right)^n \mathbf{\Phi}_{\rm rf} & ,(n \le 1) \\ \left(\bar{K}_+^{(\rm dmp)}\right)^{(n-N_y)} \mathbf{\Phi}_{\rm tr} & ,(n \ge N_y) \end{cases}. \tag{14}$$

Here, the vectors $\mathbf{\Phi}_{\rm in}, \mathbf{\Phi}_{\rm rf}$ and $\mathbf{\Phi}_{\rm tr}$ represent the incident

wave, reflected wave and transmitted wave, respectively.

The field variable $\mathbf{\Phi}(y_{N_y+1})$ can be expressed in two ways as $\mathbf{\Phi}(y_{N_y+1}) = \bar{K}_+^{(\mathrm{dmp})}\mathbf{\Phi}(y_{N_y})$ by using (14) and $\mathbf{\Phi}(y_{N_y+1}) = \bar{S}_N\mathbf{\Phi}(y_{N_y})$ by using (7). Because the tranmitted field $\mathbf{\Phi}(y_{N_y})$ can be regarded as arbitrary due to the arbitraryness of input field $\mathbf{\Phi}_{\mathrm{in}}$, we can derive

$$\bar{S}_{N_y} = \bar{K}_+^{(\mathrm{dmp})}. \tag{15}$$

This is a numerically realized ABC for output region that imposes the following conditions: (i) The travelling wave that reaches the output end is connected to a waveguide mode without any reflection. (ii) The tail of the localized wave that penetrates to the output end decreases its amplitude as the waveguide continues along the y-axis. Using the boundary condition (15), all other stepping matrices at $n < N_y$ are obtained from successive applications of (8).

Because the proposed ABC (15) involves no information about wave strengths, moments or shear forces, the condition provides a general and easily applicable expression for any system being formalized by RTM. To express ABC, the decomposing and propagating features of the matrix $\bar{K}_+^{(\mathrm{dmp})}$ are used effectively. These features can also be realized from the theoretically obtained waveguide mode [24], which is strict in the theoretical sense but the mode matching is not always strict in the numerical sense. A notable property of the condition (15) is that the non-reflection condition at the output end is strictly realized through a numerically consistent matching between the components of the scattering wave and the waveguide mode. The application scope of the proposed ABC is valid for any waveguide modes formed in a waveguide of translation invariant; a flattened mode discussed in paper I is one of those examples. The origin of the numerically matching concept can be traced back to [17]. The complex frequency-shifted PML [16], [20] also provides these same features as the proposed ABC (15). However in PML, the design of the absorbing layer needs to be changed according to governing equation; while the numerical procedure of the proposed ABC does not change when the system is changed from electromagnetic to elastodynamic except for a change in the coefficients in (2).

2.3.2 Separation of incident and scattering waves

Since the expressions $\bar{S}_0(\mathbf{\Phi}_{\mathrm{in}}+\mathbf{\Phi}_{\mathrm{rf}})$ and $\bar{K}_+^{(\mathrm{grw})}\mathbf{\Phi}_{\mathrm{in}}+\bar{K}_-^{(\mathrm{grw})}\mathbf{\Phi}_{\mathrm{rf}}$ are both for the same field $\mathbf{\Phi}(y_1)$, the reflected wave is linked to the incident wave as follows:

$$\mathbf{\Phi}_{\mathrm{rf}} = -(\bar{S}_0 - \bar{K}_-^{(\mathrm{grw})})^{-1}(\bar{S}_0 - \bar{K}_+^{(\mathrm{grw})})\mathbf{\Phi}_{\mathrm{in}}. \tag{16}$$

The reason that the waveguide is assumed to exist in $y \le y_1$ but not in $y \le y_0$ is to obtain (16). The field $\mathbf{\Phi}(y_n)$ at the arbitrary sites $n(= 1, 2, ..., N_y)$ is expressed as

$$\mathbf{\Phi}(y_n) = \bar{S}_{n-1}\cdots\bar{S}_2\bar{S}_1\bar{S}_0\mathbf{\Phi}(y_0), \tag{17}$$

with $\mathbf{\Phi}(y_0) = \mathbf{\Phi}_{\mathrm{in}} + \mathbf{\Phi}_{\mathrm{rf}}$. Specifically, considering the value at $n = N_y$, the expression for the transmitted wave is

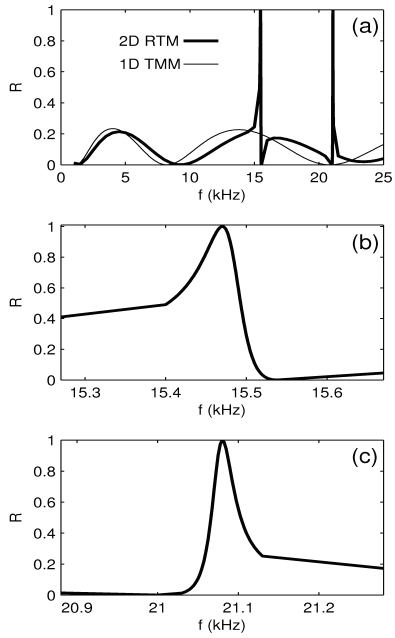

Fig. 2 Frequency dependence of the reflection rate R. (a) Wide range dependence.The thick and thin cureves indicate values calculated by two-demensional RTM and one-dimensional TMM, respectively. (b) and (c) are details of resonance curves at f = 15.47 and 21.08 kHz, respectively.

$$\mathbf{\Phi}_{\mathrm{tr}} = \bar{S}_{N_y-1}\cdots\bar{S}_2\bar{S}_1\bar{S}_0(\mathbf{\Phi}_{\mathrm{in}} + \mathbf{\Phi}_{\mathrm{rf}}). \tag{18}$$

The field vector of the incident wave, $\mathbf{\Phi}_{\mathrm{in}}$, is defined with the S_0 mode function $X_{\mathrm{sy}}(x)$ and the wave vector k_y along the y-axis as

$$\mathbf{\Phi}_{\mathrm{in}} = \{[X_{\mathrm{sy}}(x_\ell),\ ik_yX_{\mathrm{sy}}(x_\ell),\ X'_{\mathrm{sy}}(x_\ell),\ ik_yX'_{\mathrm{sy}}(x_\ell)]^T\}, \tag{19}$$

where $X'_{\mathrm{sy}}(x) = \frac{d}{dx}X_{\mathrm{sy}}(x)$. Explicit expressions of $X_{\mathrm{sy}}(x)$ and k_y are given in paper I, but the outline of S_0 mode can be seen in later Fig.3 (b) and Fig.4 (b).

When the equations (2) are gathered for all index n, and regarded as simultaneous equations for $\mathbf{\Phi}(y_n)$, they provide another method that is compatible to FEM for the scattering problem. The boundary conditions on the scattering wave are expressed with stepping matrices and the space mesh is expressed with the rectangular elements. Details on the compatibility between RTM and FEM is presented in Appendix B. For electromagnetic systems, the compatibility is not always complete because the integration region of functional is chosen as a narrower region; however the freedom to choose the integration region provides a method to improve the discretization accuracy [6].

2.4 Reflection and transmission rates

As shown in paper I, the energy flux $\mathbf{J} = [J_x, J_y]^T$, which is the energy flow per unit length and unit time, is defined by

$$\mathbf{J} = \mathbf{s}\dot{u} - M\nabla\dot{u}, \tag{20}$$

where the super dot, $\dot{}$, indicate time derivative, the field variables are not expressed in complex forms, $\mathbf{s}$ and M are shear force vector and moment tensor, respectively. The details of definitions are seen in paper I.

The steady energy flux along the y-axis is given by the mean value of the component J_y over one period $2\pi/\omega$ and over the waveguide width $|x| \le a/2$. Because the incident, reflection and transmission waves in the input or output region take the wave guide mode with the mode functions $X_{\rm in}(x)$, $X_{\rm rf}(x)$ and $X_{\rm tr}(x)$, respectively, the mean energy flux J_α ($\alpha =$ in, rf, tr) is expressed as

$$J_\alpha = \mathrm{Re}\Big[\frac{k_y\omega}{2}\int_{-a/2}^{a/2}\Big[X_\alpha\{2(k_y^2 - k_{\rm m}^2)X_\alpha - (1+\nu)X_\alpha''\} + (1-\nu)X_\alpha' X_\alpha'\Big]\frac{dx}{a}\Big], \tag{21}$$

where k_y is the wave number along the y-axis. Using these flux expressions, the reflection rate R and transmission rate T are defined by

$$R = \frac{J_{\rm rf}}{J_{\rm in}},\ T = \frac{J_{\rm tr}}{J_{\rm in}}. \tag{22}$$

3. Resonant scattering of flexural waves

3.1 System parameters

The configuration of the system is shown in Fig. 1. At the centre of an acoustic waveguide, the plate thickness is thinned from both sides, forming a step-wise structure that acts as a scatterer. The width a and thickness b of the waveguide are a = 16 mm and b = 1.0 mm, respectively. The length and thickness of the scattering region are 20 mm (= $d_{\rm sct}$) and 0.5 mm (= $b/2$), respectively. Both lengths of the side waveguides are $L_{\rm buff}$ = 8 mm. Therefore, the ends of the simulation domain are at $y_{\rm in} = -L_{\rm buff}$(= -8 mm) and $y_{\rm out} = d_{\rm sct} + L_{\rm buff}$ (= 28 mm). The numbers of spatial segments are N_x = 15 and N_y = 30, which means the step sizes are h_x= 1.067 mm and h_y=1.200 mm, respectively. The plate material is supposed to be aluminium, and the material constants are chosen as follows: Young's modulus E = 71 GPa, Poisson's ratio ν = 0.32 and mass density $\rho = 2.7\times10^3$ kg/m^3.

3.2 Reflection enhancement by resonance

3.2.1 Resonance curves

Figure 2 shows the frequency dependence of the reflection rate R , where the incident wave is assumed to be the symmetric S_0 mode given by (19). Because the system conserves energy, the transmission rate T is obtained by $T = 1 - R$. In Fig. 2 (a), the thick curves are obtained by the proposed RTM of the two-dimensional theory. Since

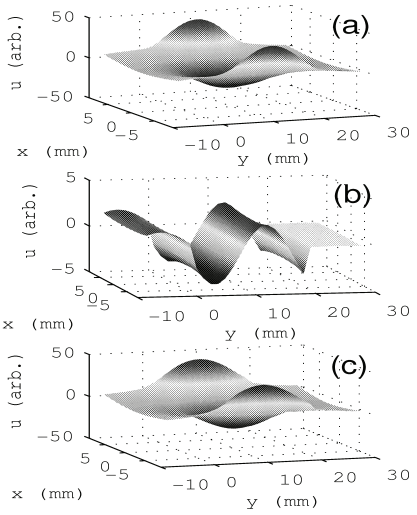

Fig. 3 Forms of scattering wave and its decomposed components at the resonance frequency f = 15.47 kHz. (a) Displacement caused by the whole scattering wave, (b) extracted travelling wave and (c) localized wave.

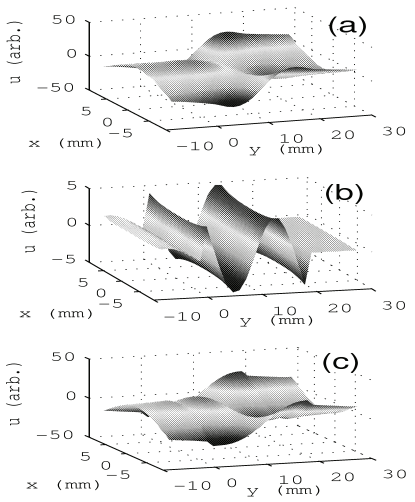

Fig. 4 Forms of a scattering wave and its decomposed components at the resonance frequency f = 21.08 kHz. (a) Displacement caused by the whole scattering wave, (b) extracted travelling wave and (c) localized wave.

the one-dimensional theory is occasionally used to design a waveguide plate [26], the result obtained by the transfer matrix method (TMM) according to the one-dimensional Euler-Bernoulli model [21] is also shown (thin curve). In the low frequency region, the thick and thin curves quite well agree, but the discrepancies appear in the high frequency region because of the difference in dimensionality. Specifically, two resonant variations appear, causing the drastic discrepancies; those resonances are captured by the two-dimensional theory but not by the one-dimensional theory.

Figures 2 (b) and (c) show that the reflection rate R is

enhanced and takes the value of unity at the frequencies of 15.47 and 21.08 kHz, respectively. The peaks of the resonance curves are asymmetric under inversion of the horizontal axis. This asymmetry is a typical feature of Fano resonance [23], which is traditionally discussed in quantum mechanical systems; it is caused by interactions between continuum energy levels and an isolated energy level. The validity of the proposed weak-form discretization scheme and RTM for analysing Fano resonance in a quantum system is already shown in [27]. In the present elastodynamic system, the state responsible for the Fano resonance is the localized wave that is induced in the scattering region.

3.2.2 Separation of localized wave from scattering waves

The localized wave causing the resonance can be extracted with the proposed RTM. The eigenvectors $[\mathbf{\Phi}_q\ \mathbf{\Psi}_q]^T$ (q = 1,2, ..., $8(N_y+1)$) serve as the bases of the $8(N_y+1)$-dimensional space which is composed of serially aligned column vectors $[\mathbf{\Phi}(y_n)\ \mathbf{\Phi}(y_{n+1})]^T$. The travelling and dampening behaviours of the eigenmodes are determined by whether the wave constant η_q is purely imaginary. The wave constant is derived from the eigenvalue λ_q as $\eta_q = \log(\lambda_q)/h_y$.

Figures 3 and 4 show the scattering and separated waves at the resonance frequencies. The travelling and localized waves are separated by using the following procedure: (i) Using the vector obtained from (17), the extended field vector $\mathbf{\Phi}_{ex}(y_n)$ of dimension $8(N_x+1)$ is composed such that $\mathbf{\Phi}_{ex}(y_n) = [\mathbf{\Phi}(y_n)\ \mathbf{\Phi}(y_{n+1})]^T$. (ii) The extended field vector $\mathbf{\Phi}_{ex}(y_n)$ is projected onto the subspace that is generated by the linear combination of the travelling waveguide modes defined by the eigenvalue problem (11). The travelling wave is composed from the first $4(N_x + 1)$-dimensional vector of the projected $\mathbf{\Phi}_{ex}(y_n)$. (iii) The localized wave component is obtained by subtracting the travelling wave from the whole scattering wave.

Panels (a), (b) and (c) in Figs. 3 and 4 show the whole scattering wave, travelling wave and localized wave, respectively. In Panel (b), the travelling wave, which is composed of the input and reflected waves, appears in the input region, $y < 0$, and no transmitted wave appears in the output region, $y > d_{sct}$(= 20 mm). This means that the reflection is enhanced by resonance, and the reflection rate reaches a maximum at $R = 1$. The wave components shown in Panels (c) occupy the scattering region, $0 < y < d_{sct}$, and have outgoing dampening wave tails that reach to the ends of the simulation domain. Although the wave tails are prominent in Fig. 4 (c), no wave disturbance appears near the boundary because perfect absorption is realized by ABC (15).

3.3 Comparison of localized wave to eigenmode

To investigate whether any eigenmode exits at the resonance frequencies obtained by RTM, the eigenvalue problem of the waveguide system is solved by FEM according to an elastodynamic equation [28]. To consider a realistic situation in the experiment, the FEM system is assumed to have finite length and to be three-dimensional. Therefore, the obtained eigenmode reflects small but finite interference caused by reflections from the ends of the simulation domain.

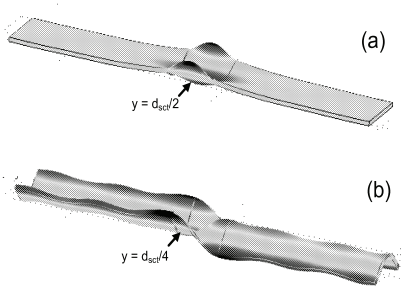

Fig. 5 The localized waves obtained by FEM analysis. Eigenfrequenies are (a) f=15.2 kHz and (b) f = 21.6 kHz. Arrows indicate points on y-axis for Fig. 6.

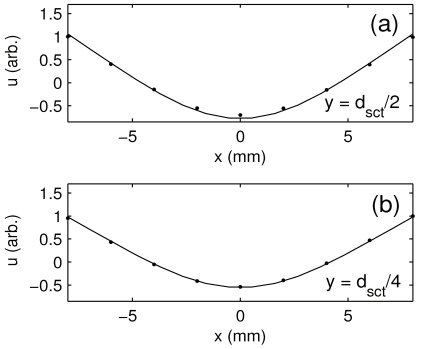

Fig. 6 Comparison of the cross sections of wave shapes along the x-axis obtained from two-dimensional RTM (solid curve) and three-dimensional FEM (dots). (a) Displacements at $y = d_{sct}/2$ obtained from Figs. 3 (c) and 5 (a). (b) Displacements at $y = d_{sct}/4$ obtained from Figs. 4 (c) and 5 (b).

Figure 5 shows the localized waves obtained from the FEM eigenmode analysis. The free boundary condition was imposed on all plate surfaces. The waveguide lengths of the input and output region were set to be relatively long such as 60 mm and 70 mm to suppress the tail amplitudes of penetrating waves that reach to the simulation boundaries. The two lengths were not same to prevent amplitude enhancements caused by superposition of reflected waves. The material constants and geometrical dimensions, except the waveguide lengths, are the same as those given in Sec. 3.1. A summary of FEM parameters is as follows: all elements were tetrahedral, the number of elements was 5171, the interpolation functions were quadratic Lagrange polynomials and the problem solver was UMFPACK.

The eigenfrequencies were found to be (a) 15.2 kHz and (b) 21.6 kHz, compared to those obtained by RTM (Fig. 2), the differences are smaller than 2.5%. Furthermore, both wave shapes are similar to those in Fig. 3 (c) and 4 (c). Figure 6 compares the wave forms along the x-axis. The dots are the displacements obtained from the three-dimensional FEM at $y = d_{sct}/2$, $d_{sct}/4$ and $z = 0$; The displacements in

Fig. 6 are scaled so that their maximum is unity. The solid curves are the wave forms from Fig. 3 (c) and 4 (c) which were scaled to fit the dots with the least squares method. The root mean squares is 4.66×10^{-2} in Fig.6 (a) and 1.62×10^{-2} in Fig.6 (b). The curves and dots well agree with each other and the agreement convinces us that RTM is effective in extracting the localized wave.

The wave shapes in Fig. 6 can be regarded as a type of the S_1 mode. The S_1 mode is the symmetric waveguide mode possessing secondary minimum deformation energy, whose definition is given in paper I. The localized waves in Fig. 5 (a) and (b) are thought to appear as a result of the enhancement caused by multiple reflections when the length d_{sct} of the scattering region is almost equal to half or all of the wave length of the S_1 mode, respectively.

In Fig. 5 (b), many of the penetrating wave tails reach to the ends of the simulation domain. This is the reason why FEM requires long input and output waveguide regions. In contrast, RTM does not require a long waveguide because of ABC, and an effective calculation is possible without using any absorption layers.

4. Conclusions

Because flexural waves are governed by a fourth-order differential equation and dampening/growing modes exist in acoustic waveguides, a localized wave tends to appear around the scattering region and induces resonance with the incident wave. By considering the symmetry of the coefficients in the difference equation, the RTM formulation is extended and applied to the resonant scattering problem of flexural waves on an acoustic waveguide made of an inhomogeneous elastic plate. This is the first application of RTM to a system that is subject to a differential equation of order higher than two. The results obtained in this study can be summarized as follows.

1. Extension of RTM to a system governed by a fourth-order differential equation.
2. Proposal of method to separate travelling and localized waves from a scattering wave.
3. Prediction of enhanced reflection caused by the resonance between the incident and localized waves.

We are planning to verify the resonant scattering of elastic waves and report the results in near future.

References

[1] J. A. Appelbaum and D. R. Hamann, "Self-consistent electronic structure of solid surfaces", Physical Review B, vol.6, no.6, pp.2166-2177, Sept. 1972.
[2] K. Hirose and M. Tsukada: "First-principles calculation of the electronic structure for a dielectrode junction system under strong field and current", Physical Review B, vol.51, no. 8, pp. 5278- 5290. 1995.
[3] H. Kato, M. Kitani and H. Kato, "Recursive transfer method as an accurate numerical method to analyze the scattering of the electromagnetic wave", IEICE Trans. Electron. (Japanese Edition), vol.J94-C, pp.1-9, 2011.
[4] H. Kato and Y. Kanno, "An analysis on Microwave Absorption of the Catalyst in a Thermal Decomposition Reaction by the Recursive Transfer Method", Japanese Journal of Applied Physics, vol.47, no. 6, pp. 4846-4850, 2008.
[5] H. Kato, M. Kitani and H. Kato, "Proposal of recursive transfer method as an accurate numerical method for microwave scattering problem", Proc. Asia-Pacific Radio Science Conference, Japan, no. BEFKc-2, Sept. 2010.
[6] H. Kato and H. Kato, "New formulation for the recursive transfer method using the weak form theory framework and its application to microwave scattering", IEICE Trans. fundamentals, vol. E96-A, no. 12, pp.2698-2708, 2013.
[7] F. Y. Hajj, H. Kobeisse and N. R. Nassif, "On the numerical solution of shroedinger's radial equation", Journal of Computational Physics, vol. 16, pp. 150-159, 1974.
[8] H. Kato and H. Kato, "An application of recursive transfer method to flexural waves I: A discretization scheme using weak form theory and waveguide modes on inhomogeneous static plates", IEICE Trans. fundamentals, vol. E97-A, pp.1075-1085, 2014.
[9] Daniel Royer and Eugene Dieulesaint, Elastic Waves in Solids II: Generation, Acousto-optic Interaction, Applications, Chap. 5, Springer, Berlin, 2000.
[10] K. Yamanouchi, Elastic device technology, Ohmsha, Tokyo 2004 (Japanese edition).
[11] B. A. Auld, Acoustic fields and waves in solids (volume II), Chap. 10, Wiley Interscience, New York, 1973.
[12] K. Yamazaki, T. Yamaguchi and H. Yamaguchi, "Modulation of Young's modulus of poly(methyl methacrylate) nano beam", Japanese Journal of Applied Physics, vol. 46, no. 49, pp. L1225-L1227, 2007.
[13] K. F. Graff, Wave motion in elastic solids, chp. 4, Oxford Univ. Press, London 1975.
[14] S. Timoshenko, and S. Woinowsky-Krieger, Theory of plate and shell (2nd ed.), chap. 4, McGraw-Hill, New York, 1959.
[15] J. P. Berenger, "A perfect matched layer for the absorption of electromagnetic waves", Journal Computational Physics, vol. 114, Issue 2, pp.185-200, 1994.
[16] J. M. Jin and D. J. Rilley, Finite Element analysis of antennas and arrays, Chap. 3, John Wiley & Sons, Hoboken, 2009.
[17] R L. Higdon, "Absorbind boundary conditon for difference approximation to the multi-dimensional wave equation", Mathematics of Computation vol. 47, no. 176, pp. 437-459, 1986.
[18] F. D. Hastings, J. B. Schneider and S. L. Broschat, "Application of the perfectly matched layer (PML) absorbing boundary condition to elastic wave propagation", Journal of Acoustic Society of America, vol. 100, issue 5, pp. 3061-3069, 1996.
[19] Q. Liu and J. Tao, "The perfectly matched layer for acoustic waves in absorptive media", J. Acoust. Soc. Am., vol. 102, issue 4, pp. 2072-2082, 1997.
[20] M. Kuzuoglu and R. Mitta, "Frequency dependence of the constitutive parameters of causal perfectly matched anisotropic absorbers", IEEE Microwave and Guided Wave Letters, vol. 6, iss. 12, pp. 447-449, 1996.
[21] C. Vemula, A. N. Norris, G. D. Cody, "Attenuation of waves in plates and bars using a graded impedance interface at edges", Journal of sound and vibration, vo. 191, no. 1, pp. 107-127, 1996.
[22] A. E. Miroshnichenko, "Fano resonances in nanoscale structures", Reviews of Modern Physics, vol. 82, no. 3, pp.2257-2298, 2010.
[23] U. Fano, "Effects of configuration interaction on intensities and phasesshifts", Physical Review, vol. 124, pp. 1866-1878, 1961.
[24] Z. Lou, J. M. Jin, "An accurate waveguide port boundary condition for the time-domain finite-element method", IEEE Transactions on Microwave Theory and Technology, vol. 53, no. 9, pp. 3014-3023, 2005.

[25] D. K. Ferry and S. M. Goodnick, Transport in nanostructures, Chap.2, Cambridge Univ. Press, Cambridge 1977.
[26] K. Yoneyama, Y. Shibata and Y. Matsumura, "Air blower using travelling space generated between two resonantly-driven plates", Proc. 2010 JSME Conf. on Robotics and Mechatronics (Japanese Edition), no. 1P1-A21, Japan, June 2010.
[27] H. Kato and H. Kato, "Weak-form discretization, waveguide boundary conditions and extraction of quasi-localized waves causing Fano resonance", IEICE Trans. fundamentals, vol. E97-A, 2014.(in printing).
[28] E. Kaussel, Fundamental solutions in elastodynamics, Cambridge Univ. Press, New York 2006.
[29] P. Šolín, Partial differential equations and the finite element method, Wiley & Sons, Hoboken, 2006.

Appendix A: Accuracy of the plane wave expression

If the elastic plate is infinite and flexural waves are free from the restriction caused by side fringes, the solution for the difference equation (2) can be found analytically. Using the analytic expression, the accuracy of the RTM solution is evaluated in this appendix.

A plane wave in an infinitely extended homogenous plate with a uniform thickness takes the following form:

$$u(x,y) = e^{\kappa y}. \tag{A·1}$$

Here, κ is the propagation constant whose analytic form is given by $\kappa = \pm k_{\rm dg}, \pm ik_{\rm pr}$, where the wave numbers $k_{\rm dg}$ and $k_{\rm pr}$ are defined by $k_{\rm dg} = \sqrt{(k_{\rm EB}^4 + k_{\rm m}^4)^{1/2} - k_{\rm m}^2}, k_{\rm pr} = \sqrt{(k_{\rm EB}^4 + k_{\rm m}^4)^{1/2} + k_{\rm m}^2}$ with $k_{\rm EB} = (\rho b\omega^2/D)^{1/4}$ and $k_{\rm m} = (\rho I\omega^2/2D)^{1/2}$.

Because the coordinates can be chosen so as to have $u_x = 0$ and $u_{xy} = 0$ for the plane wave, the third and fourth components of the discrete state $\mathbf{U}_{n\ell}$ of (5) vanish and the difference equation (2) reduces to a two-dimensional form with the vector $\mathbf{u}(y) = [u(y)\ u_y(y)]^T$ as follows:

$$c_{\rm hom}\mathbf{u}(y_{n-1}) + b_{\rm hom}\mathbf{u}(y_n) + a_{\rm hom}\mathbf{u}(y_{n+1}) = 0. \tag{A·2}$$

Here, the size of the coefficient matrices $c_{\rm hom}$, $b_{\rm hom}$ and $a_{\rm hom}$ is 2×2. In Appendix of paper I, two-dimensional vectors $\mathbf{l}_n(\zeta)$ ($\zeta = (y - h_y n)/h_y$, n = -1, 0, 1) are introduced as interpolation functions. Using the interpolation functions $\mathbf{l}_n(\zeta)$, we can defined the coefficients as follows:

$$A_n = \int_{y_n - h_y}^{y_n + h_y} dy \left(\frac{d\mathbf{l}_0}{dy}^T \begin{bmatrix} 0 & 0 \\ 0 & 1 \end{bmatrix} \frac{d\mathbf{l}_n}{dy} - \mathbf{l}_0^T \begin{bmatrix} k_{\rm EB}^4 & 0 \\ 0 & 2k_m^2 \end{bmatrix} \mathbf{l}_n \right). \tag{A·3}$$

Then, the coefficients in (A·2) can be found such as $c_{\rm hom} = A_{-1}$, $b_{\rm hom} = A_0$ and $a_{\rm hom} = A_1$.

If the flexural wave is a plane wave, it can be expressed as $\mathbf{u}(y_n) = e^{\kappa h_y n}\mathbf{u}_{\rm m}$ and the corresponding vector $\mathbf{\Phi}_n = [\mathbf{u}(y_{n-1})\ \mathbf{u}(y_n)]^T$ satisfies this equation:

$$\begin{bmatrix} c_{\rm hom} & \frac{1}{2}b_{\rm hom} \\ O_2 & I_2 \end{bmatrix} \mathbf{\Phi} = -\lambda \begin{bmatrix} \frac{1}{2}b_{\rm hom} & a_{\rm hom} \\ -I_2 & O_2 \end{bmatrix} \mathbf{\Phi} = 0. \tag{A·4}$$

Here, $\lambda = e^{\kappa h_y}$, and the matrices I_2 and O_2 are the 2×2 identity matrix and zero matrix, respectively. Solving the equation as an eigenvalue problem with eigenvalue λ and expanding the expression $\kappa = \log(\lambda)/h_y$ up to terms of h_y^4, we can find the following expression for κ:

$$\kappa = \begin{cases} \pm ik_{\rm pr}(1 - \frac{\epsilon}{2880}k_{\rm EB}^4 h_y^4 + \cdots) & \text{, travelling wave} \\ \pm k_{\rm dg}(1 - \frac{\epsilon}{2880}k_{\rm EB}^4 h_y^4 + \cdots) & \text{, localized wave} \end{cases}, \tag{A·5}$$

where ϵ is a constant that approaches unity in the limit $k_{\rm m} \to 0$. Although flexural waves are assumed to be plane wave, the error of RTM is bounded within an order of magnitude of h_y^4. The accuracy is equivalent to that of the original RTM that is formulated through Numerov's method for second-order differential equations [7].

Appendix B: Compatibility of RTM and FEM

The proposed RTM formulated by the weak form discretization scheme is compatible with the FEM procedure. When the waveguide boundary condition expressed by the stepping matrices $\bar{K}_{\pm}^{\rm (dmp)}$ and $\bar{K}_{\pm}^{\rm (grw)}$ is used to separate the input, reflection and transmission waves, the scattering problem can be transformed into the FEM framework.

According to (14), the vectors $\mathbf{\Phi}(y_{-1})$ and $\mathbf{\Phi}(y_0)$ can be expressed as $\mathbf{\Phi}(y_{-1}) = \left(\bar{K}_+^{\rm (dmp)}\right)^{-1}\mathbf{\Phi}_{\rm in} + \left(\bar{K}_-^{\rm (grw)}\right)^{-1}\mathbf{\Phi}_{\rm rf}$ and $\mathbf{\Phi}(y_0) = \mathbf{\Phi}_{\rm in} + \mathbf{\Phi}_{\rm rf}$. Here, the site y_{-1} is out of the simulation domain by one step, but it can be expressed with the vector at y_0 by eliminating the term $\mathbf{\Phi}_{\rm rf}$ as follows:

$$\mathbf{\Phi}(y_{-1}) = \bar{K}_-^{\rm (grw)}\mathbf{\Phi}(y_0) - (\bar{K}_-^{\rm (grw)} - \bar{K}_+^{\rm (dmp)})\mathbf{\Phi}_{\rm in}, \tag{A·6}$$

where the relations $\left(\bar{K}_+^{\rm (dmp)}\right)^{-1} = \bar{K}_-^{\rm (grw)}$ and $\left(\bar{K}_-^{\rm (grw)}\right)^{-1} = \bar{K}_+^{\rm (dmp)}$ were used. This is new expression for the boundary condition at the input end.

Using (14) again, another boundary condition at the output end can also be derived,

$$\mathbf{\Phi}(y_{N_y+1}) = \bar{K}_+^{\rm (dmp)}\mathbf{\Phi}(y_{N_y}). \tag{A·7}$$

The scattering problem is subject to the simultaneous equations composed of (2) with $n = 0, 1, 2, ..., N_y$. Using the boudary conditon (A·6) and (A·7), the extra vectors $\mathbf{\Phi}(y_{-1})$ and $\mathbf{\Phi}(y_{N_y+1})$ appearing at $n = 0$ and N_y can be eliminated as follows:

$$\left(\bar{c}_0\bar{K}_-^{\rm (grw)} + \bar{b}_0\right)\mathbf{\Phi}(y_0) + \bar{a}_0\mathbf{\Phi}(y_1) = \left(\bar{c}_0\bar{K}_-^{\rm (grw)} - \bar{K}_+^{\rm (dmp)}\right)\mathbf{\Phi}_{\rm in}, \tag{A·8}$$

$$\bar{c}_{N_y}\mathbf{\Phi}(y_{N_y-1}) + \left(\bar{b}_{N_y} + \bar{a}_{N_y}\bar{K}_+^{\rm (dmp)}\right)\mathbf{\Phi}(y_{N_y}) = 0. \tag{A·9}$$

Equations (2), (A·8) and (A·9) can be used to analyse the scattering problem in the waveguide. These equations are equivalent to the simultaneous equations used in FEM with a rectangular space mesh and cubic Hermite elements. Note that the boundary condition is expressed with stepping matrices, which is realized for the first time not only with the RTM framework but also with the weak-form discretization scheme.